Lecture Notes on

Astrophysics

Kevin Zhou kzhou7@gmail.com

These notes cover introductory astrophysics. The primary sources were:

- Carroll and Ostlie, An Introduction to Modern Astrophysics. The canonical undergraduate introduction, requiring only mechanics and electromagnetism. A massive book giving a clear overview of all subfields of astrophysics, though references to experiments are a bit out of date.
- Maoz, Astrophysics in a Nutshell.

The most recent version is here; please report any errors found to kzhou7@gmail.com.

Contents

1	Stars	1
	.1 Stellar Interiors	
	.2 Radiative Transport	5
	.3 Stellar Energy Transport	6
	.4 Stellar Models	12
2	Telescopes	18
3	Γhe Solar System	2 2
4	Galaxies	2 3
5	Compact Objects	2 4

1 Stars

1.1 Stellar Interiors

We begin with a simple hydrostatic model for the internal structure of a star.

• The basic parameters of our Sun are

$$M_{\odot} = 2 \times 10^{30} \,\mathrm{kg}, \quad R_{\odot} = 7 \times 10^8 \,\mathrm{m}, \quad \rho_{\odot} = 1400 \,\mathrm{kg/m}^3.$$

• We assume spherical symmetry, and let P(r) be the pressure at a given radius, M(r) be the mass within radius r, and $\rho(r)$ be the density at radius r. The equation of hydrostatic equilibrium is

$$\frac{dP}{dr} = -\rho g, \quad g(r) = \frac{GM(r)}{r^2}.$$

• By definition, M(r) satisfies the mass conservation equation

$$\frac{dM}{dr} = 4\pi r^2 \rho.$$

To go further, we need an equation of state to solve for the pressure.

• For most settings we can use the ideal gas law, which can be written in the form

$$P = \frac{\rho k_B T}{\mu m_H}$$

where m_H is the mass of a hydrogen atom, and μ is the mean molecular weight, i.e. the average mass of a free particle in the gas, in units of m_H .

• For a collection of neutral atoms, with molecular weights A_j and mass fractions X_j ,

$$\frac{1}{\mu} = \sum_{j} \frac{X_j}{A_j}.$$

The atoms may also be ionized, in which case the electrons contribute to the number of free particles. Assuming full ionization, if z_j is the atomic number, then

$$\frac{1}{\mu} = \sum_{j} \frac{X_j}{A_j} (1 + z_j).$$

For intermediate ionizations, one can use the Saha equation.

• In astrophysics, it is conventional to separate the mass into the mass fractions of hydrogen X, helium Y, and "metals" Z, where metals include everything else, giving

$$\frac{1}{\mu} = X + \frac{1}{4}Y + \left\langle \frac{1}{A} \right\rangle Z, \quad \frac{1}{\mu} = 2X + \frac{3}{4}Y + \left\langle \frac{1+z}{A} \right\rangle Z.$$

For a typical young star, $X=0.70,\,Y=0.28,\,Z=0.02,\,\langle 1/A\rangle\approx 1/15,\,{\rm and}\,\,\langle (1+z)/A\rangle\approx 1/2.$

• We may also have to include a pressure contribution due to radiation pressure,

$$P = \frac{\rho k_B T}{\mu m_H} + a T^4, \quad a = \frac{4\sigma}{c} = 7.566 \times 10^{-16} \,\text{J m}^{-3} \,\text{K}^{-4}$$

where a is called the radiation constant. In smaller stars, this contribution is negligible, but for larger stars it becomes dominant in the hot cores.

Note. We can get a very crude estimate of the pressure at the core by taking the star to be uniform,

$$P_c \sim \frac{GM_{\odot}\rho_{\odot}}{R_{\odot}} \sim 3 \times 10^{14} \,\mathrm{N/m^2}.$$

At the core, we have complete ionization, which implies $\mu \approx 0.62$ given the above parameters. Then the ideal gas law gives

$$T_c \sim 1.4 \times 10^7 \, {\rm K}.$$

The value for the pressure is too small by about a factor of 100 because it does not account for the increased density at the core. On the other hand, for the temperature the errors in the pressure and density roughly cancel out, giving a result reasonably close to detailed solar models. At this temperature, the radiation pressure is about 10^{-3} times the total pressure.

In order to solve the hydrostatic equilibrium equation, we need to know the dependence of temperature on radius, which in turn requires an understanding of stellar energy sources.

• In the 19th century, it was thought that stars were powered by the gravitational potential energy released during contraction. For a uniform star of mass M and radius R,

$$U \sim -\frac{3}{5} \frac{GM^2}{R}$$

which implies that the Sun could have only been burning at its current luminosity for about 10^7 years, which was incompatible with geological results. The available energy that could be released by chemical reactions was even smaller.

• The resolution was the discovery of nuclear fusion processes, which typically take place at MeV energies, far above the eV scale of chemical reactions. For example, suppose the Sun burns 10% of its hydrogen into helium. This releases 0.7% of the mass-energy, so the energy released is

$$E \sim (0.1)(0.007)M_{\odot}c^2 \sim 10^{44} \,\mathrm{J}$$

which is enough to power the Sun for 10^{10} years.

• Nuclear fusion processes can't be explained by classical physics alone. For two protons to get as close as their radius, $r \sim 1 \, \text{fm}$, we require a temperature

$$T \sim \frac{ke^2}{k_B r} \sim 10^{10} \, \mathrm{K}$$

which is much higher than the core temperature.

• As a very rough estimate of when quantum tunneling effects allow fusion, suppose we only require the protons to get as close as their de Broglie wavelength $\lambda = h/p$. Then we have

$$k_B T \sim \frac{ke^2}{\lambda} \sim \frac{p^2}{2m_p} \sim \frac{\hbar^2}{\lambda^2 m_p}.$$

Solving for λ and plugging it back in gives

$$T \sim \frac{k^2 e^4 m_p}{\hbar^2 k_B} \sim 10^7 \,\mathrm{K}$$

which is more reasonable.

• In order to compute nuclear reaction rates, we need the cross section $\sigma(E)$. As a rough starting point, we again suppose that a reaction occurs if two particles overlap within a de Broglie wavelength, $\lambda \propto 1/\sqrt{E}$. Then the cross section should have the rough dependence

$$\sigma(E) \sim \lambda^2 e^{-aU/E}$$

where the first term is for the geometrical cross-section, and the exponential term is from the tunneling. The potential barrier height is $U \propto \sqrt{E}$. Thus, we conventionally write

$$\sigma(E) = \frac{S(E)}{E} e^{-b/\sqrt{E}}$$

where S(E) is a slowly varying function of energy which captures the detailed nuclear physics, such as resonance peaks. Another detail which is important in practice is that electrons can screen the nuclear charges, reducing the potential barrier height.

• Given the cross sections for each reaction and the momentum distribution functions, we can compute the rate ϵ_{ij} of energy production per unit mass due to fusion of species i and j. For heuristic discussion, it is often useful to approximate it in some narrow range of densities and temperatures as a power law,

$$\epsilon_{ij} \approx \epsilon_0 X_i X_j \rho^{\alpha} T^{\beta}$$

where $\alpha = 1$ for two-body reactions (since one factor of density is included in the definition of ϵ), and β can range from 1 to over 40. The temperatures are traditionally expressed in terms of $T_n = T/(10^n \,\mathrm{K})$.

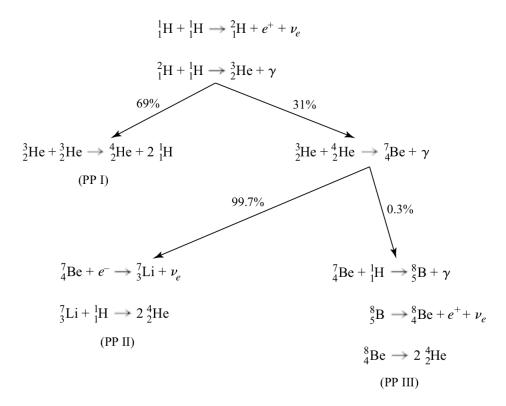
• The contribution of a mass dm to the total luminosity is $dL = \epsilon dm$, where ϵ is the total rate of energy released per unit mass, including both gravitational and nuclear contributions. Thus,

$$\frac{dL}{dr} = 4\pi r^2 \rho \epsilon$$

where the interior luminosity L(r) is defined as the total energy generated within radius r.

We now give some examples of stellar nuclear reactions.

• In the proton-proton chain, protons are fused into ⁴He nuclei. As shown below, this can occur through three distinct branches, with branching ratios shown appropriate for the Sun.



The first step is one of the slowest, because it is a weak process. The proton-proton chain is the dominant fusion mechanism in the Sun, and near the core temperatures of $T_6 \approx 15$, the temperature scaling is $\beta \approx 4$, which is relatively weak.

• Helium-4 is also produced in the CNO cycle, which uses carbon, nitrogen, and oxygen as catalysts. The main branch is shown below.

$${}^{12}_{6}C + {}^{1}_{1}H \rightarrow {}^{13}_{7}N + \gamma$$

$${}^{13}_{7}N \rightarrow {}^{13}_{6}C + e^{+} + \nu_{e}$$

$${}^{13}_{6}C + {}^{1}_{1}H \rightarrow {}^{14}_{7}N + \gamma$$

$${}^{14}_{7}N + {}^{1}_{1}H \rightarrow {}^{15}_{8}O + \gamma$$

$${}^{15}_{8}O \rightarrow {}^{15}_{7}N + e^{+} + \nu_{e}$$

$${}^{15}_{7}N + {}^{1}_{1}H \rightarrow {}^{12}_{6}C + {}^{4}_{2}He.$$

Near $T_6 = 15$, the CNO cycle has a strong temperature dependence, $\beta \approx 20$. It starts to dominate for stars slightly heavier than the Sun.

- As protons are fused to helium over the lifetime of a star, the mean molecular weight μ decreases, so in the absence of any other changes, the pressure would decrease, causing the star to shrink. After shrinking in size by a small amount, the central temperatures and densities rise again, reestablishing equilibrium.
- Eventually, stars heat up further and burn helium into carbon in the triple alpha process,

$${}^4_2\mathrm{He} + {}^4_2\mathrm{He} \leftrightarrow {}^8_4\mathrm{Be}, \quad {}^8_4\mathrm{Be} + {}^4_2\mathrm{He} \leftrightarrow {}^{12}\mathrm{C}_* \to {}^{12}_6\mathrm{C} + 2\gamma.$$

The first reaction has a bidirectional arrow because ${}^8_4\text{Be}$ decays very quickly, usually before it is hit with another helium nucleus. As a result, the reaction is effectively three-body, and the reaction rate scales as $(\rho Y)^3$, so $\alpha = 2$. The star denotes an excited state of carbon; the presence of this resonance is essential for enough carbon to be produced, and was in fact predicted by Hoyle before it was discovered in accelerator experiments. There is a very strong temperature dependence near $T_8 = 1$ of $\beta \approx 41$.

• As this process continues, carbon can also react with helium to form oxygen, and oxygen can react with helium to form neon,

$${}^{12}_{6}\mathrm{C} + {}^{4}_{2}\mathrm{He} \rightarrow {}^{16}_{8}\mathrm{O} + \gamma, \quad {}^{16}_{8}\mathrm{O} + {}^{4}_{2}\mathrm{He} \rightarrow {}^{20}_{10}\mathrm{Ne} + \gamma.$$

However, at typical helium burning temperatures, the Coulomb barrier prevents further reactions from occurring.

• If a star is sufficiently massive, even higher central temperatures can be obtained, leading to carbon and oxygen burning near 10⁹ K, producing a wide variety of heavier nuclei. Some of these reactions are even endothermic, i.e. they are driven by their entropy production.

1.2 Radiative Transport

To complete our simple hydrostatic model, we must describe how energy is transported through the star. Typically, conduction is negligible, so we focus on radiation and convection. For radiation, we begin with a description of the radiation field.

• The radiation distribution is described by the specific intensity

$$I_{\lambda} = \frac{dE}{d\lambda \, dt \, dA \, \cos \theta \, d\Omega}.$$

Specifically, this means the energy per wavelength per time that passes through an area dA, with the light's momentum pointing within a solid angle $d\Omega$. The factor of $\cos \theta$ in the numerator, where θ is the angle between the direction of the light and the normal to the area, reflects the fact that the projection of the area in the light's direction of travel is only $dA \cos \theta$.

• The mean intensity is the average over all directions,

$$\langle I_{\lambda} \rangle = \frac{1}{4\pi} \int I_{\lambda} \, d\Omega.$$

For isotropic radiation, $I_{\lambda} = \langle I_{\lambda} \rangle$.

• The specific energy density is the energy density per wavelength,

$$u_{\lambda} = \frac{dE}{d\lambda \, dV}.$$

Since the intensity of plane wave radiation divided by c is the energy density,

$$u_{\lambda} = \frac{1}{c} \int I_{\lambda} \, d\Omega.$$

• For blackbody radiation, u_{λ} is given by Planck's law,

$$u_{\lambda} = \frac{4\pi}{c} B_{\lambda} d\lambda = \frac{8\pi h c/\lambda^5}{e^{hc/\lambda k_B T} - 1}, \quad I_{\lambda} = B_{\lambda}$$

where we used isotropy. It is also useful to express quantities per unit frequency,

$$u_{\nu} = \frac{4\pi}{c} B_{\nu} = \frac{8\pi h \nu^3 / c^3}{e^{h\nu/k_B T} - 1}, \quad I_{\nu} = B_{\nu}.$$

Integrating over all frequencies gives $u = aT^4$, where a is the radiation constant.

• The specific radiative flux F_{λ} is the net energy per wavelength per time that passes through an area dA,

$$F_{\lambda} = \frac{dE}{d\lambda \, dt \, dA} = \int I_{\lambda} \cos \theta \, d\Omega = \int_{0}^{2\pi} d\phi \int_{0}^{\pi} d\theta \, I_{\lambda} \cos \theta \sin \theta.$$

Note that the $\cos \theta$ factor accounts the direction that the energy passes through the area, so that an isotropic radiation field has $F_{\lambda} = 0$.

- Optical instruments typically measure the specific intensity due to a source, where the area dA is their aperture. However, in practice the stars that telescopes look at often cannot be resolved, so they only see the radiative flux.
- This leads to different scalings in the two different cases. For a star that is resolved, the specific intensity does not depend on how far away it is: the specific radiative flux falls off as $1/r^2$, but the solid angle the light is spread over also falls as $1/r^2$. But for a star that is not resolved, the solid angle is fixed by diffraction, so only the former factor matters.
- The pressure in the z-direction is the rate of transfer of z-momentum in the z-direction. Since the momentum of a photon is its energy divided by c, the radiation pressure per wavelength is

$$P_{z,\lambda} = \frac{1}{c} \int I_{\lambda} \cos^2 \theta \, d\Omega$$

where θ is the angle to the z-axis, and the two factors of $\cos \theta$ are for the momentum component and velocity component. Assuming the radiation is isotropic, the pressure is

$$P = \frac{4\pi}{3c} \int I_{\lambda} \, d\lambda = \frac{u}{3}.$$

Next, we consider how radiation propagates out of a stellar atmosphere, which is also important to understanding the appearance of stars.

• We consider following the intensity of a ray of wavelength λ as it travels a distance ds through a region of density ρ . Then

$$dI_{\lambda} = -\kappa_{\lambda} \rho I_{\lambda} ds + i_{\lambda} \rho ds$$

where κ_{λ} is the opacity, or absorption coefficient, and j_{λ} is the emission coefficient.

• To simplify this, we define the source function and optical depth,

$$S_{\lambda} = \frac{j_{\lambda}}{\kappa_{\lambda}}, \quad d\tau_{\lambda} = -\kappa_{\lambda} \rho \, ds$$

where the optical depth is zero at the exterior of the star, and increases inward. Then

$$\frac{dI_{\lambda}}{d\tau_{\lambda}} = I_{\lambda} - S_{\lambda}.$$

This is the transfer equation.

- If the matter is locally in thermal equilibrium, then $S_{\lambda} = B_{\lambda}$ by Kirchoff's law. In this case, the transfer equation just states that the radiation field ends up at the same temperature as the matter, $I_{\lambda} = B_{\lambda}$, as expected. It becomes nontrivial for stellar atmospheres, where temperature varies with height.
- Since the radii of stars are huge, we assume a plane-parallel atmosphere, i.e. that properties of the atmosphere depend only on z. We also switch variables to the vertical optical depth,

$$\tau_{\lambda,v} = \tau_{\lambda} \cos \theta$$

where θ is the angle of the ray to the z-axis. Finally, for simplicity we assume a gray atmosphere, where the absorption and emission coefficients are independent of wavelength.

• Integrating over wavelengths gives

$$\cos\theta \, \frac{dI}{d\tau_v} = I - S.$$

Integrating this over solid angles gives

$$\frac{dF_{\rm rad}}{d\tau_{\rm re}} = 4\pi(\langle I \rangle - S), \quad S = B = \frac{\sigma T^4}{\pi}$$

where we used the assumption of local thermal equilibrium. This result expresses conservation of energy: an accumulation of radiation energy, due to a gradient in $F_{\rm rad}$, is due to the difference between the local intensity and the source function.

• On the other hand, first multiplying both sides by $\cos \theta$ and integrating over solid angle gives

$$\frac{dP_{\rm rad}}{d\tau_v} = \frac{1}{c}F_{\rm rad}$$

where P_{rad} is the radiation pressure in the z-direction. This tells us that the net flow in radiation F_{rad} is the result of a radiation pressure gradient.

• For simplicity, we consider an equilibrium stellar atmosphere, where no net energy is added or subtracted from the radiation field. In this case,

$$F_{\rm rad} = F_{\rm surf} \equiv \sigma T_e^4, \quad \langle I \rangle = S$$

where T_e is the surface temperature. Note that we do not have I = S, since there is a net outward flow of radiation. Integrating our radiation pressure equation gives

$$P_{\rm rad} = \frac{1}{c} F_{\rm rad} \tau_v + C$$

where C is a constant of integration.

• At this point, we're stuck, because the actual values of quantities like $F_{\rm rad}$ and $P_{\rm rad}$ depend on the detailed orientation dependence of I_{λ} . In the Eddington approximation, we assume that I_{λ} has constant values $I_{\rm in}$ and $I_{\rm out}$ for all directions with a negative/positive z-component. Then

$$\langle I \rangle = \frac{I_{\mathrm{out}} + I_{\mathrm{in}}}{2}, \quad F_{\mathrm{rad}} = \pi (I_{\mathrm{out}} - I_{\mathrm{in}}), \quad P_{\mathrm{rad}} = \frac{2\pi}{3c} (I_{\mathrm{out}} + I_{\mathrm{in}}) = \frac{4\pi}{3c} \langle I \rangle.$$

• At the top of the atmosphere, $\tau_v = I_{\rm in} = 0$, which implies $\langle I(\tau_v = 0) \rangle = F_{\rm rad}/2\pi$. Plugging this into the radiation pressure equation fixes the value of C, giving

$$\frac{4\pi}{3}\langle I\rangle = F_{\rm rad}\left(\tau_v + \frac{2}{3}\right).$$

Finally, plugging in the known values of $\langle I \rangle$ and $F_{\rm rad}$ gives

$$T^4 = \frac{3}{4}T_e^4 \left(\tau_v + \frac{2}{3}\right)$$

which expresses the temperature dependence of the stellar atmosphere.

• The surface temperature T_e is the temperature we infer by looking at the intensity of radiation released from the surface of the star. The above derivation tells us that, for a gray atmosphere, the surface temperature is actually achieved at optical depth $\tau_v = 2/3$. Equivalently, this is the typical depth that the photons we actually see come from.

We now combine these formal results with physical context for stellar atmospheres.

- In the photosphere, the mean free path of a typical visible photon is about 150 km, while the temperature scale height (the distance over which the temperature changes by a factor of e) is $H_T = 700 \,\mathrm{km}$. Thus, we can see only a relatively small fraction into the photosphere.
- Since the source function S_{λ} depends only on temperature, the opacity κ_{λ} determines the strength of the coupling between the matter and radiation, for both emission and absorption. In reality, κ_{λ} has sharp peaks. Therefore, as a beam propagates out of the atmosphere, encountering lower temperatures as it goes, the intensity I_{λ} decreases the most for wavelengths with high κ_{λ} . This leads to the observed spectral absorption lines of stars.
- Many distinct physical mechanisms contribute to the opacity.
 - Bound-bound transitions occur when electrons in atoms, ions, or molecules absorb a photon and transition between orbitals. These transitions have sharp dependence on λ , so they lead to spectral lines. Often, the absorption of a photon is accompanied by immediate reemission of a photon of the same energy; this only contributes to scattering.
 - Bound-free absorption, also known as photoionization, occurs when a photon ionizes an atom. Since this can occur for a wide range of energies, it contributes to the continuum opacity.
 - Free-free absorption occurs when a free electron near an ion absorbs a photon, transferring some of its momentum to the ion. This also contributes to the continuum opacity.
 - Momentum and energy conservation imply that an isolated electron only can scatter photons.
 Depending on the frequency range, this is called Thomson or Compton scattering. Electrons bound to nuclei also can mediate Rayleigh scattering, which is broad in spectrum.

As required by thermodynamics, all of the absorption processes have reverse emission processes: for bound-free absorption it is recombination, and for free-free absorption it is Bremsstrahlung.

- We have listed several sources of scattering, but for simplicity, we have neglected scattering in the above formalism; it would appear as a contribution of the form $dI_{\lambda} \supset \kappa_{\lambda,s} \rho \langle I_{\lambda} \rangle ds$. Scattering is not essential for our purposes, though it is needed to explain many phenomena, such as the blueness of the sky due to Rayleigh scattering.
- The sources of opacity above have a complicated temperature dependence. For cooler stars, such as our Sun, photoionization of the loosely bound H⁻ ion dominates the continuum opacity. For warmer stars, photoionization of H and free-free absorption dominate. At every higher temperatures, electron scattering and the photoionization of He dominate.
- Since it is inconvenient to carry around the full frequency dependence, we often work in terms of the Rosseland mean opacity,

$$\frac{1}{\overline{\kappa}} = \frac{\int d\nu \, \frac{1}{\kappa_{\nu}} \frac{\partial B_{\nu}(T)}{\partial T}}{\int d\nu \, \frac{\partial B_{\nu}(T)}{\partial T}}.$$

Typically, $\overline{\kappa} \propto \rho/T^{3.5}$, and any opacity with this dependence is called a Kramer opacity law.

• A concrete consequence of our formalism is "limb darkening". The edge/limb of the Sun appears darker than the center, because we can see only into a depth $\tau \approx 2/3$. For the "edge-on" view at the limb, this corresponds a smaller vertical optical depth, and hence a lower temperature.

1.3 Stellar Energy Transport

With this background, we are finally ready to treat energy transport inside stars. We begin with the case where radiation is the dominant energy transport mechanism.

• Our earlier treatment of radiative transport was suited for the stellar atmosphere; now we will derive a slightly different version for the interior. We allow general frequency-dependence of the opacity. Integrating over solid angle but not frequency, we have

$$\frac{dP_{\mathrm{rad},\nu}}{d\tau_{v,\nu}} = \frac{1}{c}F_{\mathrm{rad},\nu}.$$

Since we have spherical symmetry, we work in terms of the radius, $d\tau_{v,\nu} = -\kappa_{\nu}\rho dr$, giving

$$F_{\mathrm{rad},\nu} = -\frac{c}{\kappa_{\nu}\rho} \frac{dP_{\mathrm{rad},\nu}}{dr}$$

where $P_{\rm rad}$ is the radiation pressure in the radial direction.

• Integrating over frequencies gives

$$F_{\rm rad} = -\frac{c}{\rho} \int \frac{d\nu}{\kappa_{\nu}} \frac{dP_{{\rm rad},\nu}}{dr} = -\frac{c}{\rho \overline{\kappa}} P_{\rm rad}, \quad \overline{\kappa} = \frac{\int (d\nu/\kappa_{\nu}) dP_{{\rm rad},\nu}/dr}{\int d\nu dP_{{\rm rad},\nu}/dr}.$$

This definition of $\overline{\kappa}$ coincides with the Rosseland mean, because

$$\frac{dP_{\mathrm{rad},\nu}}{dr} \propto \frac{dB_{\nu}}{dr} = \frac{\partial B_{\nu}(T)}{\partial T} \frac{dT}{dr}.$$

• As we saw previously, $I_{\text{out}} - I_{\text{in}}$ is a constant in the Eddington approximation, but both I_{out} and I_{in} are extremely large in the hot stellar interior. Thus, we can approximate the radiation field as isotropic, giving $P_{\text{rad}} = aT^4$. Also, we substitute $F_{\text{rad}} = L/4\pi r^2$ where L is the interior luminosity. This gives the temperature gradient

$$\frac{dT}{dr} = -\frac{3}{4ac} \frac{\overline{\kappa}\rho}{T^3} \frac{L}{4\pi r^2}$$

when radiative transport dominates.

Note. The total optical thickness of a star, from its core to its outer atmosphere, is extremely large. Let the mean free path be d and the solar radius be R, so the optical depth is $\tau \sim R/d$. Then up to some philosophical quibbles about the identity of photons, each photon experiences $N \sim \tau^2$ scattering events to exit the star in its random walk. This is a factor of τ larger than the time it would take with no scattering at all. That in turn is the factor by which the core luminosity $R^2T_c^4$ is reduced to the surface luminosity $R^2T_s^4$, so $\tau \sim (T_c/T_s)^4$, an enormous quantity. The total time t is on the order of a million years.

It is difficult to treat convection quantitatively, since it is often turbulent, and the characteristic sizes of convection cells are not small compared to the star itself. Instead, we will give a qualitative treatment, determining when it occurs and only estimating its impact.

• We define the pressure scale height

$$\frac{1}{H_P} = -\frac{1}{P}\frac{dP}{dr} = \frac{P}{\rho g}.$$

In the interior of the star, we have $H_P \sim R_{\odot}/10$.

• The adiabatic sound speed in the body of the Sun is

$$v_s = \sqrt{\frac{\gamma P}{\rho}} \sim 4 \times 10^5 \,\mathrm{m/s}.$$

The time required for a sound wave to traverse the Sun's diameter is about an hour; this is the typical period of stellar pulsations.

• Consider a parcel of gas which rises in the radial direction adiabatically. During this process, all of its thermodynamic properties change simultaneously, and by the ideal gas law,

$$\frac{dP}{dr}\bigg|_{\rm ad} = -\frac{P}{\mu}\frac{d\mu}{dr}\bigg|_{\rm ad} + \frac{P}{\rho}\frac{d\rho}{dr}\bigg|_{\rm ad} + \frac{P}{T}\frac{dT}{dr}\bigg|_{\rm ad}.$$

We emphasize that these are properties of the bubble, not the surrounding star.

• For simplicity, we take μ to be constant, removing the first term. In an adiabatic process, $P \propto \rho^{\gamma}$, so the second term becomes $(1/\gamma)(dP/dr)$. Finally, using the equation of hydrostatic equilibrium and the ideal gas law again gives

$$\left. \frac{dT}{dr} \right|_{\text{ad}} = \left(1 - \frac{1}{\gamma} \right) \frac{T}{P} \frac{dP}{dr} \right|_{\text{ad}} = -\left(1 - \frac{1}{\gamma} \right) \frac{\mu m_H}{k_B} \frac{GM}{r^2} = -\frac{g}{C_P}$$

where C_P is the heat capacity at constant pressure per unit mass.

• If the actual temperature gradient exceeds this,

$$\left| \frac{dT}{dr} \right| > \left| \frac{dT}{dr} \right|_{\text{ad}}$$

then it is said to be superadiabatic. As a convective bubble rises, it will maintain the same pressure as the surrounding material, but a different density, $\rho \propto 1/T$. For a superadiabatic temperature gradient, the bubble will be hotter than its surroundings and hence lighter, and therefore be propelled further upward by the buoyant force.

• A simple equivalent form of the superadiabatic criterion is

$$\frac{d\log P}{d\log T}<\frac{\gamma}{\gamma-1}.$$

We assume an ideal monatomic gas, $\gamma = 5/3$.

- Convection occurs when the opacity is high, since this increases |dT/dr|, or when the specific heat is high, since this decreases $|dT/dr|_{ad}$. For typical stars, this tends to be true in their atmospheres. It turns out that convection is a very effective heat transfer mechanism, so when convection happens at all, it dominates and sets $|dT/dr| \approx |dT/dr|_{ad}$.
- We can get a rough understanding of why this is the case using the "mixing length theory". We parametrize a superadiabatic temperature gradient by

$$\left. \frac{dT}{dr} \right|_{\text{ad}} = (1 - \delta) \frac{dT}{dr}.$$

We suppose that a rising bubble travels a "mixing length"

$$\ell = \alpha H_P$$

before dissipating and thermalizing with its surroundings. Here, α is an O(1) number, though we can't derive why without more detailed fluid dynamics.

• The heat transferred per volume of bubble is the heat capacity per volume times the temperature difference,

$$q \sim (C_P \rho) \ell \delta \frac{dT}{dr}.$$

In the steady state, convection cells will form, where material is continuously carried upward in hot bubbles, cool, and then sinks down. Then the radiative flux due to convection is

$$F_c \sim q \overline{v}_c$$

where \overline{v}_c is the typical radial bubble velocity.

• We estimate \overline{v}_c by noting that the buoyant force is responsible for accelerating the bubble. Therefore, averaging over the mixing length, the work-kinetic energy theorem gives

$$\rho \overline{v}_c^2 \sim \left(\rho \frac{\ell \delta}{T} \frac{dT}{dr}\right) g\ell$$

where the term in parentheses is the typical density difference.

• Combining all of these results gives

$$F_c \sim \rho C_P \left(\frac{k_B}{\mu m_H}\right)^2 \left(\frac{T}{g}\right)^{3/2} \alpha^2 \left(\delta \frac{dT}{dr}\right)^{3/2}.$$

Assuming that convection accounts for all heat transfer in the Sun's convection zone, $F_c = L/4\pi r^2$, and plugging in typical numbers gives

$$\delta \sim 10^{-6}$$
, $\overline{v}_c \sim 50 \,\text{m/s} \sim 10^{-4} \,v_s$.

Thus, even a tiny superadiabatic temperature gradient and a slow bubble velocity suffices. Intuitively, this is plausible because radiative transport is *also* very slow, as the photons randomly walk, with only a very slight bias towards the surface.

• The details of convection are much more complicated than can be accounted for in this model. For example, near the surface of the star, the convective velocity can approach the sound speed. Also, the typical timescales for bubble motion are comparable to dynamic timescales, such as for stellar pulsation. A detailed account of convection requires numeric simulation.

1.4 Stellar Models

In this section we consider full models of stars. However, to calibrate our models, we need to know the masses of the stars. The main method to accomplish this is to see the gravitational interactions of binary stars, which make up most of the stars in the sky. These are classified by how they are detected.

- In a visual binary, both stars can be resolved independently. If the distance to the stars is known, the linear separation can be calculated. Measuring the center of mass location and the period of the orbit yields the masses, via Kepler's third law. An optical double is a "fake" visual binary, where two unrelated stars happen to lie along the same line of sight.
- If one member of a binary is much brighter than the other, so that the fainter one cannot be seen, but the brighter one is close enough to track its motion, then the existence of the fainter star can be inferred from the oscillatory motion of the brighter. This is an astrometric binary. With only partial information, we cannot get both stellar masses, but we can bound them.
- In an eclipsing binary, one star periodically passes in front of the other, blocking some of the light. The "light curves" can provide information about the relative effective temperatures and radii of each star.
- We can also infer the motion of binary stars by the periodically varying Doppler shifts of their spectral lines. The contributions of the two stars can be distinguished by their opposite Doppler shifts. This is a spectrum binary. Given the period and the velocities, we can again infer the masses by Kepler's third law.
- If one of the stars is too faint to see, then we have a spectroscopic binary, where the presence of the other star is inferred from the oscillations of the spectral lines of the first.
- We don't provide explicit formulas because in all cases, the data analysis can get complex. For example, the stars can orbit in a plane with arbitrary orientation, which must be inferred from astrometry, and stars can rotate and pulsate, confusing spectroscopic measurements.

• Exoplanets were first discovered in 1995, and most have been discovered at a rapid pace since. Exoplanet detection is similar in principle to detecting binaries, but requires greater precision. We again look for light curves indicating a transiting exoplanet, or tiny stellar wobbles, measured either astrometrically or from Doppler shifts. To date, most discovered exoplanets are "hot Jupiters", i.e. heavy and close-orbiting, but this may just be a selection effect. Currently, the Gaia telescope is taking a detailed astrometric and spectroscopic survey of about 1% of the astronomical bodies in the galaxy, and expects to detect many exoplanets.

Note. Consider a uniform gas cloud of mass M, radius R, and temperature T. It will begin to collapse into a star only if the inward gravitational force can exceed the outward pressure. These forces balance when their contributions to the energy are comparable,

$$\frac{GM^2}{R} \sim Nk_BT.$$

Therefore, collapse occurs if the mass M exceeds the Jeans mass

$$M_J \sim \frac{k_B T R}{G m}$$

where m is the mass of a gas particle. We can equivalently write this criterion in terms of a critical length or critical density,

$$R_J \sim \sqrt{\frac{k_B T}{G m \rho}}, \quad \rho_J \sim \frac{1}{M^2} \left(\frac{k_B T}{G m}\right)^3.$$

We used this same criterion in a somewhat different context in the notes on Cosmology.

Next, we discuss general stellar models.

• We have accumulated a series of differential equations that govern the star,

$$\frac{dP}{dr} = -\frac{GM\rho}{r^2}, \quad \frac{dM}{dr} = 4\pi r^2 \rho, \quad \frac{dL}{dr} = 4\pi r^2 \rho \epsilon$$

and

$$\frac{dT}{dr} = -\begin{cases} \frac{3}{4ac} \frac{\overline{\kappa}\rho}{T^3} \frac{L}{4\pi r^2} & \text{radiation dominated} \\ (1 - \frac{1}{\gamma}) \frac{\mu m_H}{k_B} \frac{GM}{r^2} & \text{ideal adiabatic convection dominated} \end{cases}.$$

In the static case, ϵ is sourced entirely by nuclear fusion; we can also introduce time dependence, in which case ϵ includes the change in gravitational potential energy.

- In order to get a concrete result, we need constitutive relations, i.e. expressions for the parameters $P, \overline{\kappa}$, and ϵ in terms of ρ , T, and the composition. In practice, the ideal gas law plus radiation pressure gives a decent estimate for P. The calculations of $\overline{\kappa}$ and ϵ require detailed atomic and nuclear physics, respectively.
- The solution must be fixed by boundary conditions at the center and surface of the star. A simple set is

$$M(0) = L(0) = 0, \quad T(R_*) = P(R_*) = \rho(R_*) = 0$$

where R_* is the star's radius. More realistically, the temperature, pressure, and density never fall exactly to zero; instead we should match onto the stellar atmosphere.

- The Vogt–Russell theorem is a uniqueness theorem for these differential equations. It states that once the total mass, composition structure, and constitutive relations are specified, all other features of the solution are uniquely determined.
- The numeric integration itself can be set up in a variety of ways. In a Eulerian code, the radius r is discretized, turning the differential equations in r into difference equations. In a Lagrangian code, we convert the differential equations into ones over M, e.g. dP/dr = (dP/dM)(dM/dr), and discretize M. Lagrangian codes are especially useful for tracking stellar evolution, because over the course of a star's lifetime, the radius varies by orders of magnitude while the mass does not.
- Since boundary conditions are specified at both the center and surface, we typically start from both ends and integrate inward. Multiple iterations are required to make the solutions match at the fitting point.

The situation simplifies dramatically if we make the restrictive simplifying assumption that the pressure depends only on the density, and not the temperature. In this case, the dT/dr and dL/dr equations can be ignored entirely, and we can use the dP/dr and dM/dr equations to determine the density profile of the star.

• By combining these equations, we have

$$\frac{1}{r^2}\frac{d}{dr}\left(\frac{r^2}{\rho}\frac{dP}{dr}\right) = -4\pi G\rho.$$

In fact, since $(1/\rho)dP/dr$ is the radial gravitational acceleration $-d\Phi/dr$, this equation is simply the spherically symmetric form of Poisson's equation.

• Lane and Emden considered the "polytropic" equation of state $P = K\rho^{1+1/n}$, which yields

$$\frac{n+1}{n}\frac{K}{r^2}\frac{d}{dr}\left(r^2\rho^{(1-n)/n}\frac{d\rho}{dr}\right) = -4\pi G\rho.$$

• To analyze this equation, it is useful to switch to dimensionless variables,

$$\rho(r) = \rho_c(D_n(r))^n, \quad \lambda_n = \sqrt{(n+1)\frac{K\rho_c^{(1-n)/n}}{4\pi G}}, \quad r = \lambda_n \xi$$

which gives the Lane-Emden equation,

$$\frac{1}{\xi^2} \frac{d}{d\xi} \left(\xi^2 \frac{dD_n}{d\xi} \right) = -D_n^n.$$

We normalize the solution setting $D_n(0) = 1$, so that ρ_c is the central density.

• To solve the equation, we need two boundary conditions. The first is that

$$D_n(\xi_1) = 0$$
 where ξ_1 is the first zero of $D_n(\xi)$.

For the second, note that we have implicitly assumed ρ is nonsingular at the core. Then the gravitational field goes to zero there, so dP/dr goes to zero, which implies

$$\left. \frac{dD_n}{d\xi} \right|_{\xi=0} = 0.$$

• Given a solution for $D_n(\xi)$, the mass of the star is

$$M = 4\pi\lambda_n^3 \rho_c \int_0^{\xi_1} \xi^2 D_n^n d\xi.$$

This can be simplified by using the Lane-Emden equation inside the integral, giving

$$M = -4\pi\lambda_n^3 \rho_c \, \xi_1^2 \frac{dD_n}{d\xi} \bigg|_{\xi = \xi_1}.$$

• Some analytic solutions to the Lane–Emden equation are

$$D_n(\xi) = \begin{cases} 1 - \xi^2/6 & n = 0\\ \sin \xi & n = 1\\ (1 + \xi^2/3)^{-1/2} & n = 5 \end{cases} \quad \eta = 0 \quad \pi = 0$$

$$\pi \quad n = 1.$$

$$\infty \quad n = 5$$

Since the radius of the star diverges for n = 5, the physically valid values are $0 \le n \le 5$, where n = 5 works since the mass is finite.

- Several value of n have physical significance.
 - The limit $n \to 0$ is a bit singular, but corresponds to an incompressible object, with uniform density. In this limit, D_0 tracks the pressure, rather than the density. This doesn't make any sense for stars, but it is a crude model for the Earth.
 - The case n = 3/2 corresponds to $P \propto \rho^{5/3}$, which corresponds to an adiabatic monatomic gas. It also corresponds to nonrelativistic degeneracy pressure, and hence white dwarfs.
 - The case n=3, or $P \propto \rho^{4/3}$, corresponds to relativistic degeneracy pressure, and hence describes white dwarfs on the verge of collapse.
- The case n=3 appears in a simple stellar model, the Eddington standard model. We suppose that essentially all of the mass and luminosity are concentrated right at the center of the star, so M(r) and L(r) can be treated as constants. We also treat the opacity as constant. Then

$$\frac{dP}{dr} \propto -\frac{\rho}{r^2}, \quad \frac{dP_{\rm rad}}{dr} \propto -\frac{\rho}{r^2}$$

where in both equations we only drop constants. Thus, radiation pressure makes up a constant fraction of the total pressure, so the ratio of radiation pressure to gas pressure is constant, so

$$\frac{T^4}{\rho T} = \text{const}, \quad \rho \propto T^3.$$

This determines the temperature, giving

$$P \propto P_{\rm rad} \propto T^4 \propto \rho^{4/3}$$

which corresponds to n = 3. Despite its simplicity, the Eddington standard model gives reasonable results, when compared to much more complicated models.

We now qualitatively describe the main sequence, which encompasses most stars in the universe.

• Main sequence stars burn hydrogen in their cores, and lie along the range

$$M \in [0.1, 40] M_{\odot}, \quad L \in [10^{-3}, 10^{6}] L_{\odot}, \quad T_e \in [2000, 40000] K, \quad R \in [0.1, 20] R_{\odot}.$$

As the mass increases, the core temperatures and pressures increase dramatically, as do the luminosity, so that more massive stars on the main sequence live for a shorter time. The surface temperature only varies over a few orders of magnitude, but this is sufficient to dramatically affect their appearance.

• At the surface of a star, the radiation pressure gradient and total pressure gradient are

$$\frac{dP_{\rm rad}}{dr} = -\frac{\overline{\kappa}\rho}{c} \frac{L}{4\pi r^2}, \quad \frac{dP}{dr} = -G\frac{M\rho}{r^2}.$$

Since the total pressure gradient bounds the radiation pressure gradient, the luminosity is bounded by the Eddington luminosity,

$$L_{\rm Ed} = \frac{4\pi Gc}{\overline{\kappa}}M.$$

For heavier main sequence stars, the main contribution to $\overline{\kappa}$ is electron scattering, and the observed luminosities are within a factor of a few of the limit.

- For lighter main sequence stars, around the mass of the Sun, energy is primarily produced by the pp chain and the core is radiative, while the atmosphere is convective. For heavier stars, energy is primarily produced by the CNO cycle, which causes convection to also dominate in the core. Eventually, when the hydrogen is almost exhausted, the star can exit the main sequence and become a red giant.
- Note that the equations of stellar structure mostly relate monomials in the variables to each other. Therefore, in certain regimes, we can take a solution to the equations and scale it appropriately to get another solution; this is the principle of homology.
- We work in terms of the fractional mass variable x = M(r)/M. Since the mass is now a variable, we parametrize the mass distribution by r(x) instead. The principle of homology states that

$$r = M^{a_1} r_s(x)$$

where $r_s(x)$ is part of an existing solution, along with similar results for the other variables,

$$\rho(r) = M^{a_2} \rho_s(x), \quad T(r) = M^{a_3} T_s(x), \quad P(r) = M^{a_4} P_s(x), \quad L(r) = M^{a_5} L_s(x).$$

• For this to have a chance of working, we need additional assumptions about the constitutive relations. We assume the energy transport is always radiation dominated, the pressure is always dominated by the ideal gas pressure $P \propto \rho T$, and $\overline{\kappa}$ and ϵ have the dependence

$$\overline{\kappa} \propto \begin{cases} \rho/T^{3.5} & \text{low mass, Kramers opacity} \\ \text{const} & \text{high mass, electron scattering} \end{cases}, \quad \epsilon \propto \begin{cases} T^4 & \text{low mass, } pp \text{ chain} \\ T^{16} & \text{high mass, CNO cycle} \end{cases}.$$

• The four stellar equations and the equation of state yield five constraints on the five exponents $(a_1, a_2, a_3, a_4, a_5)$, which give the solutions

low mass: (1/13, 10/13, 12/13, 22/13, 71/13), high mass: (15/19, -26/19, 4/19, -22/19, 3).

In particular, the exponents a_5 for luminosity gives the mass-luminosity relation

$$L \propto \begin{cases} M^{5.5} & \text{low mass} \\ M^3 & \text{high mass} \end{cases}$$

which is actually qualitatively correct. For very low mass stars, this argument breaks down completely because the stars are convection dominated, while for very high mass stars we have $L \propto M$ as radiation pressure dominates and the Eddington limit becomes effective.

• We can combine the above results with $L \propto R^2 T_e^4$ to get a luminosity-temperature relationship,

$$L \propto \begin{cases} T_e^{4.5} & \text{low mass} \\ T_e^{8.5} & \text{high mass} \end{cases}$$

which (very) qualitatively matches the Hertzsprung–Russell diagram.

Note. The virial theorem relates the internal and potential energies of a star, using only the assumption of hydrostatic equilibrium. First, consider a star made of a monatomic ideal gas. Then the internal energy is

$$E_{\rm int} = \int \frac{3}{2} \frac{N_A}{\mu} k_B T dM = \frac{3}{2} \int \frac{P}{\rho} dM.$$

Now consider the equation of hydrostatic equilibrium.

$$\frac{dP}{dr} = -\frac{GM(r)}{r^2}\rho$$

and multiply both sides by $4\pi r^3 dr$, giving

$$\int 4\pi r^3 \frac{dP}{dr} dr = -\int \frac{GM(r)}{r} \rho(4\pi r^2) dr = E_{\text{grav}}.$$

The left-hand side can be integrated by parts, and the boundary term vanishes since P(R) = 0, so

$$E_{\text{grav}} = -\int_0^R 12\pi r^2 P \, dr = -3\int \frac{P}{\rho} \, dM.$$

Thus, we conclude $2E_{int} + E_{grav} = 0$. For a general adiabatic index, we instead have

$$3(\gamma - 1)E_{\text{int}} + E_{\text{grav}} = 0, \quad E_{\text{tot}} = \frac{3\gamma - 4}{3\gamma - 3}E_{\text{grav}}.$$

For $\gamma > 4/3$, which is typically the case, this says that stars release energy when they contract gravitationally, as expected. Note that for a relativistically degenerate gas, $\gamma = 4/3$, in which case $E_{\rm tot}$ vanishes. This is why sufficiently heavy white dwarfs are unstable against collapse.

2 Telescopes

We begin with some useful numbers for thinking about telescopes.

• If a star lies in the orbital plane of the Earth, then over a year it will oscillate with respect to the distant stars due to parallax. If the distance to the star is d, the parallax has amplitude

$$\theta = \frac{1 \text{ AU}}{d}$$
, $1 \text{ AU} = 1.496 \times 10^{11} \text{ m} = 499 \text{ s}$.

Typical astronomical angles are given in terms of arcminutes and arcseconds,

$$1' = \frac{1^{\circ}}{60}, \quad 1'' = \frac{1'}{60}.$$

• The parsec ("parallax second") is defined to be the distance d so that $\theta = 1''$, so

$$1 \text{ pc} = 3600 \text{ AU} = 3.086 \times 10^{16} \text{ m} = 3.262 \text{ yr}.$$

The angular resolution of a telescope is limited by the diffraction limit, $\Delta\theta \sim 1.22 \, \lambda/D$ where D is the aperture. As a few references for angular width:

- The moon has average angular diameter 30'.
- The resolution of the human eye is about 1'.
- The nearest stars have parallaxes that are a fraction of an arcsecond.
- For a large optical telescope, $D \sim 1 \, \mathrm{m}$ and $\lambda \sim 600 \, \mathrm{nm}$, the diffraction limit is $\Delta \theta \sim 0.15''$.
- Because of atmospheric blurring, which causes stars to visibly twinkle, ground-based telescopes have trouble resolving angles smaller than 0.5".
- The star with the largest angular diameter besides the Sun is the red giant R Doradus, which has diameter 0.05".
- The most precise astrometric measurements are made by the Gaia satellite, which can find star positions down to about $10 \,\mu{\rm as}$.
- The apparent magnitude m is a logarithmic scale for the flux of light from a star, where a difference of 5 in magnitude corresponds to a factor of 100 in flux. Historically, the brightest stars were assigned m = 1 and the dimmest visible to the naked eye were assigned m = 6.
- The total flux over all wavelengths gives the bolometric magnitude m, but there are also measures for wavelength ranges. The most common are the U, B, and V magnitude, which correspond to ultraviolet, blue, and visible light respectively. The color of a star is quantified by the color indices U B and B V. The quantity m V is called the bolometric correction.
- The apparent magnitude V=0 corresponds to a flux per frequency of

$$3640 \,\mathrm{Jy} = 3.64 \times 10^{-20} \,\mathrm{erg \, s^{-1} \, cm^{-2} \, Hz^{-1}}.$$

This roughly corresponds to an intensity

$$I \sim 100^{-V/5} 10^{-8} \,\mathrm{W/m^2} \sim 10^{10-V/5} \,\mathrm{photons/m^2 \,s}.$$

- For reference, Jupiter has m=-2, Vega has m=0, Andromeda has m=3.5, and Proxima Centauri has m=11. A good amateur telescope can see down to $m\approx 15$, automated astronomical surveys with minute-long exposures can see down to $m\approx 24$, and the Hubble space telescope with a month-long exposure time can see down to $m\approx 31$. At these extreme cases, the telescopes are simply limited by the number of incoming photons.
- The total flux is related to the luminosity of a star by

$$F = \frac{L}{4\pi r^2}.$$

The absolute magnitude M is defined as the apparent magnitude a star would have if it were at a distance 10 pc.

We now review some features of optical telescopes.

- Optical telescopes can be either reflecting or refracting. However, refracting telescopes are challenging to scale up, as they experience chromatic aberration, and require the entire volume of the lens to be clean. As a result, all leading modern optical telescopes are reflecting.
- Reflecting telescopes direct the light back in the direction it came from. A simple "prime focus" design thus requires the astronomer to physically stand inside the telescope to use it. Modern designs use secondary mirrors to extract the light.
- For large reflecting telescopes, it is essential to precisely grind the mirror. The Hubble space telescope famously experienced a multi-year delay because its mirror was too shallow by $2 \mu m$.
- Optical telescopes can be either space-based or ground-based. Ground-based telescopes are larger and cheaper, but suffer from atmospheric turbulence; as such, most are concentrated in a few calm, high-altitude sites with clear weather, such as Mauna Kea and the Chilean Andes. Telescopes also require "adaptive optics" to cancel out time-varying atmospheric effects, and "active optics" to correct distortions of the mirrors, e.g. due to thermal expansion.
- The quantum efficiency of a detector is the fraction of photons it can detect. The human eye has a quantum efficiency of 1%, and photographic plates are not much better. Astronomy has been revolutionized by the development of charge-coupled devices (CCDs), which have quantum efficiencies of nearly 100% from the soft X-ray range to the infrared.
- The largest ground-based optical/infrared telescopes are about 10 m wide. They include:
 - Gemini North and South, at Mauna Kea and Chile.
 - The Very Large Telescope (VLT), a set of four telescopes in Chile.
 - Keck I and II, and Subaru/HSC, at Mauna Kea.
 - The Large Binocular Telescope (LBT) in Arizona, the Gran Telescopio Canarias (GTC) in Spain, the Hobby-Eberly Telescope (HET) in Texas, and the Southern African Large Telescope (SALT) in South Africa.

Adjacent telescopes, such as those in the VLT array, can be combined to give better angular resolution by effectively increasing the aperture width, as described in the notes on Optics.

• There are also a few proposed larger telescopes, to see first light in the late 2020s:

- The Thirty Meter Telescope (TMT) at Mauna Kea, which is politically controversial.
- The Giant Magellan Telescope in Chile.
- The Extremely Large Telescope (ELT) in Chile, with a 40 m diameter.
- The Overwhelmingly Large Telescope (OWL), with a 100 m diameter, was proposed as a conceptual design, but isn't funded.
- The very expensive, "flagship" space-based optical telescopes are:
 - The Hubble Space Telescope, which has a 2.4 m diameter, and has produced iconic images such as the Hubble Deep Field.
 - The James Webb Space Telescope is the successor to Hubble. It has been delayed by 15 years, during which its estimated cost has increased from \$1 billion to \$10 billion.
 - Gaia is a European telescope designed for precision astrometry, surveying the Milky Way.
- There are also other telescopes/collaborations aimed specifically at surveying the sky. These have four main purposes: detecting near-Earth objects such as asteroids, detecting astrophysical transients, such as gamma ray bursts, surveying the Milky Way, and doing cosmology by measuring the matter power spectrum and the redshifts of supernova. Specific examples include:
 - CSS, Pan-STARRS, and ATLAS, for detecting near-Earth objects.
 - The Zwicky Transient Facility (ZTF) for near-Earth objects and transients.
 - The past Sloan Digital Sky Survey (SDSS) for cosmology. It will be improved upon by a variety of next generation experiments starting in the early 2020s: the Vera C. Rubin Observatory, previously known as the Large Synoptic Survey Telescope (LSST), the Dark Energy Survey, which will use the Dark Energy Camera (DECam) on a 4 m telescope in Chile, and Euclid, a European spacecraft.
- Yet more telescopes measure nearby stars precisely, to detect exoplanets; all of them are in space. Current examples include Kepler, TESS, and CHEOPS, while proposed future experiments include PLATO, ARIEL, HabEx, and LUVOIR.

Next, we very briefly review other kinds of telescopes.

- Going higher in frequency, the atmosphere strongly absorbs UV and X-rays, so these telescopes need to be in space. On the other hand, high energy gamma rays are rare and can punch through the atmosphere, so it's best for these to be ground-based.
- Gamma ray and X-ray telescopes are listed in the notes on Cosmology. For gamma ray telescopes, the relevant statistic is just the count rate. For X-ray telescopes, the standard unit is the luminosity of the Crab nebula,

$$1 \, \mathrm{crab} = 2.4 \times 10^{-8} \, \mathrm{erg \, cm^{-2} \, s^{-1}} = 2.4 \times 10^{-11} \, \mathrm{W/m^2}$$

including photons from 2 keV to 10 keV.

• Gamma ray telescopes necessarily have wide fields of view and poor angular resolution, because gamma rays can't be focused with optics like visible photons. X-ray telescopes are intermediate: it is possible to deflect X-rays by small angles, so one can build an X-ray telescope with a narrow field of view by using nested layers of mirrors, each at grazing incidence. This also applies to solar X-ray telescopes, such as axion helioscopes.

- In the absence of such optics, the incoming direction of a gamma ray or X-ray can be inferred from a track, for high energies, or from the shadow of a coded mask, if there are enough of them; this is how X-ray telescopes with wide fields of view work.
- UV telescopes have more in common with optical telescopes; in fact, many of the optical telescopes listed above can also see in the near-UV. However, going further into the UV is challenging because glass becomes transparent. Some past examples were the Extreme Ultraviolet Explorer (EUVE), Far Ultraviolet Spectroscopic Explorer (FUSE), Hopkins Ultraviolet Telescope (HUT), Galaxy Evolution Explorer (GALEX), and currently Hisaki/SPRINT-A. UV instruments are also included on the Swift Gamma-Ray Burst Mission and Hubble
- Going lower in frequency, the atmosphere is still transparent to the near-IR, and many of
 the optical telescopes listed above can also see in this range. Far-IR/microwave telescopes
 are typically space-based due to atmospheric absorption, while radio telescopes are typically
 ground-based. OST is a proposed far-IR space observatory for studying exoplanets; the Spitzer
 Space Telescope is a past one.
- Microwave telescopes are primarily used for cosmology, by measuring the CMB. Examples are:
 - The Cosmic Background Explorer (COBE), launched in 1989.
 - The Wilkinson Microwave Anisotropy Probe (WMAP), launched in 2001.
 - Planck, launched in 2009, which currently provides the best constraints on many cosmological parameters.

Note that at these frequencies and below, thermal noise is important.

- Radio telescopes can probe exotic compact objects. In addition, the 21 cm spectral line of hydrogen can be used to probe the ionization of hydrogen over the universe's history, and thus constrain cosmology.
- Radio telescopes are severely impacted by the diffraction limit, so to achieve good angular resolution, they must use extremely large apertures, combine arrays of telescopes, or use very-long-baseline interferometry (VLBI), effectively connecting telescopes thousands of miles apart. This technique was used by the Event Horizon Telescope (EHT) to image a black hole.
- Examples of specific radio telescopes include:
 - The 300 m Arecibo Observatory in Puerto Rico, completed in 1963.
 - The recently completed 500 m Aperture Spherical Radio Telescope (FAST), in China.
 - The Very Large Array (VLA) in New Mexico, and the Atacama Large Millimeter Array (ALMA) in Chile.

However, the specific names of these telescopes aren't as important, since VLBI can connect radio telescopes all across the world.

3 The Solar System

4 Galaxies

5 Compact Objects